

# A MASSIVELY PARALLEL MATRIX FREE FE-BASED MULTIGRID METHOD FOR SIMULATING THE BEHAVIOR OF HETEROGENEOUS MATERIALS USING LARGE SCALE CT IMAGES

---

Xiaodong LIU, Julien RÉTHORÉ, Ton LUBRECHT

September 23, 2020

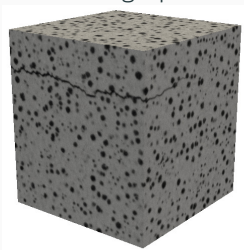
Research Institute in Civil Engineering and Mechanics (GeM)  
UMR 6183, CNRS, Centrale Nantes, Université de Nantes, France

# BACKGROUND AND MOTIVATIONS

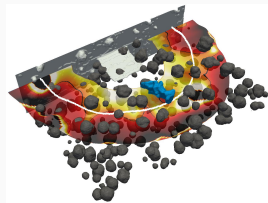
X-ray tomography opens new way to analyze materials

- 3D images  $\mu$ structure (RVE)  $\rightarrow$  computational homogenisation
- *in-situ* experiments
  - DVC: displacement / strain at the micro-scale  
microstructure  $\leftrightarrow$  structure ( geometry, BCs,...)
  - ↗ for crack / singularity

Crack in nodular graphite cast iron



PhD thesis J. Lachambre



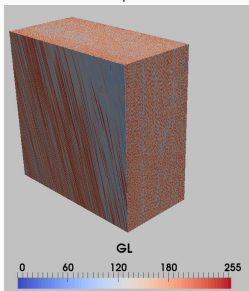
Analysis of DVC fields  
SIF, crack tip position,...

# BACKGROUND AND MOTIVATIONS

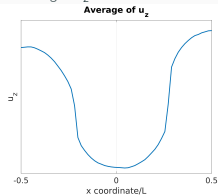
X-ray tomography opens new way to analyze materials

- 3D images  $\mu$ structure (RVE)  $\rightarrow$  computational homogenisation
- *in-situ* experiments
  - DVC: displacement / strain at the micro-scale  
microstructure  $\leftrightarrow$  structure ( geometry, BCs,...)
  - ↗ for crack / singularity

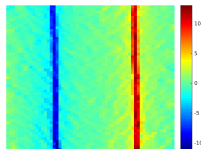
Laminate composite material



Averaged  $U_z$  on the free surface



Strain $_{xz}$  on the free surface



## BACKGROUND AND MOTIVATIONS

X-ray tomography opens new way to analyze materials

- 3D images  $\mu$ structure (RVE)  $\rightarrow$  computational homogenisation
- *in-situ* experiments
  - DVC: displacement / strain at the micro-scale  
microstructure  $\leftrightarrow$  structure ( geometry, BCs,...)
  - ↗ for crack / singularity

Usually DVC results are difficult to analyse / interpret

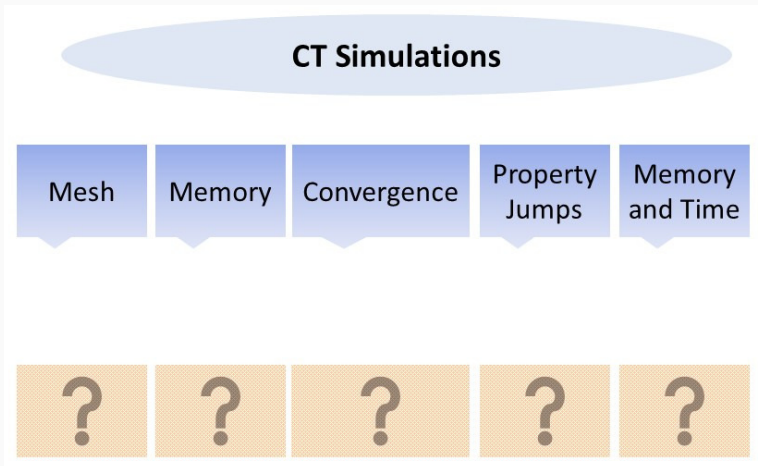
- microstructure  $\leftrightarrow$  structure
- DVC (spatial-)resolution  $\approx$  a few tens of voxels
- neither a micro displacement nor a macro displacement

$\rightarrow$  need to perform numerical simulations at the micro-scale to

- understand these interactions
- analyse the DVC results

## OBJECTIVE & QUESTIONS

Perform **automatically** numerical simulations using **large** CT images, *e.g.* 8 billion voxels, of **heterogeneous** materials.



## Well-known numerical methods:

- Finite Element Methods (**FEM**): (LENGSFELD *et al.* 1998, FERRANT *et al.* 1999)
- Fast Fourier Transform (**FFT**): (NEMAT-NASSER *et al.* 1982, SUQUET 1990)
- Finite Difference Methods (**FDM**): (GU *et al.* 2016)

LENGSFELD M., SCHMITT J., ALTER P., KAMINSKY J., LEPPEK R., *Medical engineering & physics*, 20, 515-522, 1998.

FERRANT M., WARFIELD S. K., GUTTMANN C. R., MULKERN R. V., JOLESZ F. A., KIKINIS R., *International Conference on Medical Image Computing and Computer-Assisted Intervention Springer*, 202-209, 1999

NEMAT-NASSER S., IWAKUMA T., HEJAZI M., *Mechanics of materials*, 1, 239-267, 1982.

SUQUET P., *Comptes rendus de l'Académie des sciences. Série 2, Mécanique, Physique, Chimie, Sciences de l'univers, Sciences de la Terre*, 311, 769-774, 1990.

Gu, H., Réthoré, J., Baietto, M.-C., Sainsot, P., Lecomte-Grosbras, P., Venner, C. H., Lubrecht, A. A., *Computational materials science*, 112, 230-237, 2016

Advantages of each numerical method for large scale CT simulations:

- **FEM:**
  - Abundant element types can deal with complex geometry
  - Implementation of boundary conditions is straightforward
- **FFT:**
  - Performed on the regular voxel grid
  - Efficient for **periodic** problems
- **FDM:**
  - Mesh generation is efficient (one voxel/point)
  - Smaller memory requirement

Drawbacks of each numerical method for large scale CT simulations:

- **FEM:** expensive on **Meshing** step and **relaxation** step
- **FFT:** only for **periodic** boundary condition problems
- **FDM:** boundary conditions are difficult to implement

FEM with one node = one voxel

## CT Simulations

Mesh

Memory

Convergence

Property  
Jumps

Memory  
and Time

Voxel/  
node

?

?

?

?



Thermal conduction in heterogeneous materials:

$$\begin{cases} \nabla \cdot (\boldsymbol{\alpha} \nabla T) = 0 \\ T = T_0 & \text{on } \Gamma_1 \\ T = T_1 & \text{on } \Gamma_2 \\ \boldsymbol{\alpha} \cdot \nabla T \cdot \boldsymbol{n} = 0 & \text{on the other surfaces} \end{cases}$$

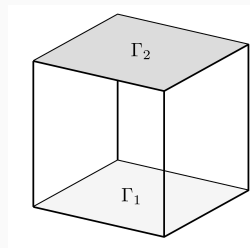


Figure 1: Boundary conditions

- $\boldsymbol{\alpha}$  is a high contrast variable coefficient ( $1 \sim 1\,000$ )

The weak form of the original equation:

$$-\int_{\partial\Omega} \boldsymbol{\alpha} \nabla T \cdot \vec{n} \varphi dS + \int_{\Omega} \boldsymbol{\alpha} \nabla T \cdot \nabla \varphi d\Omega = 0$$

which is also referred to:  $\mathbf{q}_{\text{in}} = \mathbf{q}_{\text{ex}}$  with

$$\begin{cases} \mathbf{q}_{\text{in}} = - \int_{\Omega} \boldsymbol{\alpha} \nabla T \cdot \nabla \varphi d\Omega \\ \mathbf{q}_{\text{ex}} = - \int_{\partial\Omega} \boldsymbol{\alpha} \nabla T \cdot \vec{n} \varphi dS \end{cases}$$

One voxel per elementary node, at node  $j$  with MF-FEM:

$$(q_{\text{in}})_j = - \sum_e \sum_i \sum_m \sum_{g=1}^8 w_g \nabla_m \varphi_i \alpha^g T_i \nabla_m \varphi_j$$

$\alpha^g$  is the conductivity at Gauss integration point:

$$\alpha^g = \sum_{i=1}^8 \alpha_i \varphi_i$$

Jacobi relaxation node by node without matrix assembly:

$$T_i^{iter+1} = T_i^{iter} + \omega \frac{(q_{ex} - q_{in})_i}{stiff_i}$$

$\omega$ : relaxation coefficient.

$$stiff_i = \sum_e \sum_m \sum_{g=1}^8 w_g \nabla_m \varphi_i \alpha^g \nabla_m \varphi_i$$

Matrix free FEM (MF-FEM) (HUGHES *et al.* 1983):

- Dispenses from assembling stiffness matrix: Size of stiffness matrix (**sparse**): 3.8 TB for a problem with 18 billion of DoF
- Suited for voxel conversion problems (one element type)

# PERFORMANCE OF MF-FEM

Proposed Jacobi MF-FEM for a  $129^3$  nodes spherical thermal conduction problem with a contrast of 10

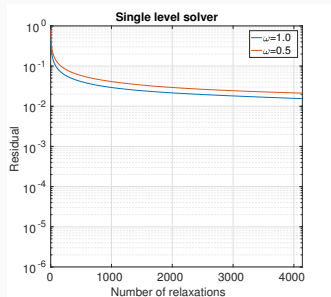


Figure 2: Convergence

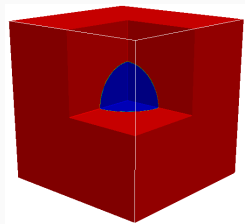


Figure 3: Spherical inclusion

A residual of  $10^{-2}$  with a cost of  $4000 W_U$   
 $W_U$  is the cost of one relaxation

## CT Simulations

Mesh

Memory

Convergence

Property  
Jumps

Memory  
and Time

Voxel/  
node

MF-FEM

?

?

?

# EFFICIENCY OF STANDARD MG METHODS

	Single level	FMG scheme
Residual achieved	$1.55 \times 10^{-2}$	$7.89 \times 10^{-6}$
Cost / $W_U$	4139	19.6

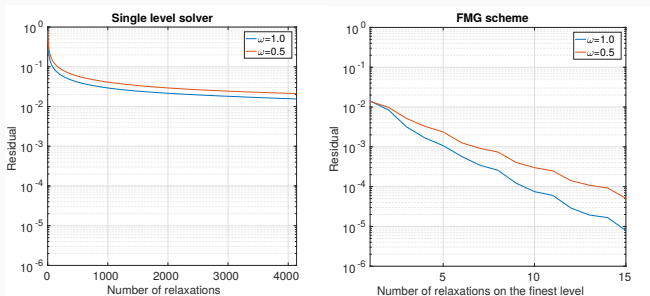


Figure 4: Convergence of single level (left) and FMG scheme (right) on a  $129^3$  nodes spherical thermal conduction problem with a contrast of 10

## CT Simulations

Mesh

Memory

Convergence

Property  
Jumps

Memory  
and Time

Voxel/  
node

MF-FEM

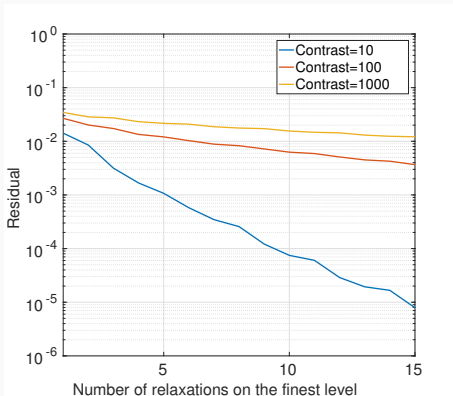
MultiGrid

?

?

# MG CONVERGENCE FOR HIGH CONTRAST

Convergence of MG on a  $129^3$  nodes spherical thermal conduction problem with different material property contrasts



Standard MG can not deal with problems with large variations



## CT Simulations

Mesh

Memory

Convergence

Property  
Jumps

Memory  
and Time

Voxel/  
node

MF-FEM

MultiGrid

Specific  
operators

?

## LIMITATION OF SERIAL COMPUTING

- memory and computational time
- $2049 \times 2049 \times 2049$  voxels  $\rightarrow$  more than  $8 \times 10^9$  nodes
- 8 billion DoF  $\rightarrow$  239 days .
- $3 \times 8$  billion DoF  $\rightarrow 3 \times 239$  days  $\approx$  2 years !!!.

Parallel computing must be implemented to avoid these difficulties

The solver has to be designed with a good parallel performance  
Jacobi is a good candidate !

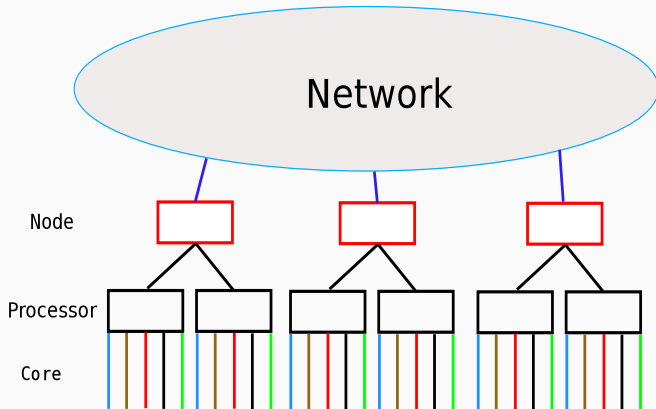


Figure 5: Architecture of Liger in ICI, Centrale Nantes

# PARALLEL PROGRAMMING

- Distributed memory:  
Message Passing Interface (MPI) on nodes
- Shared memory:  
OpenMP in node

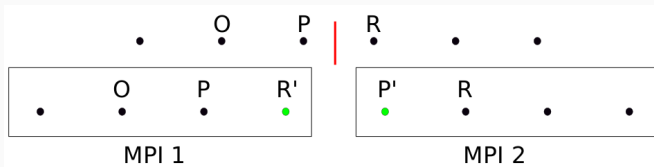
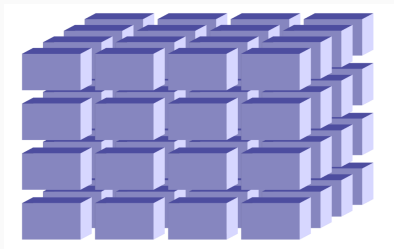


Figure 6: Ghost points

Hybrid MPI/OpenMP: several OpenMP / MPI

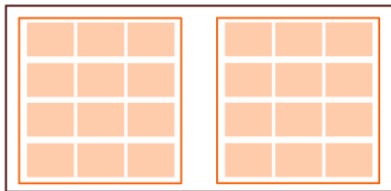


Figure 7: One node with 2 processors in Liger

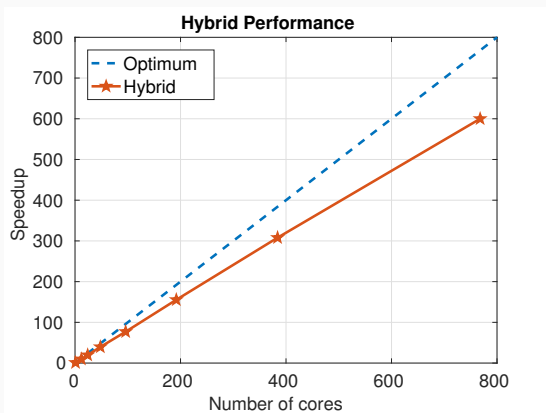
$64 \text{ MPI} \times 12 \text{ OpenMP} = 768 \text{ cores}$  (Limited at 1 000 cores for each laboratory)

Advantages of Hybrid MPI/OpenMP:

- Smaller memory requirement (fewer ghost points)
- Easier post processing (1 Output file / MPI)
- **Suited for MG methods**

## PARALLEL PERFORMANCE

The figure is obtained by solving a one billion DoF problem.



768 cores: about 80% of optimum speedup.

## CT Simulations

Mesh

Memory

Convergence

Property  
Jumps

Memory  
and Time

Voxel/  
node

MF-FEM

MultiGrid

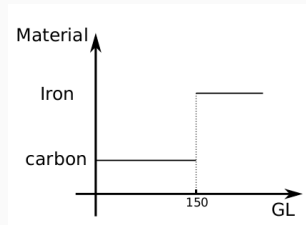
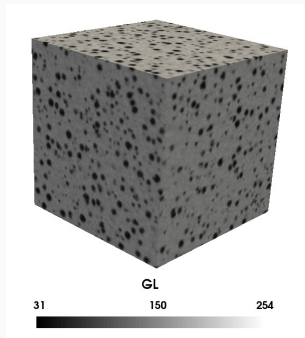
Specific  
operators

HPC

# NODULAR GRAPHITE CAST IRON IMAGE

Image obtained by RANNOU *et al.*

Region Of Interest (ROI):  $257 \times 257 \times 257$  voxels,  $\approx 50$  million DoF



where  $GL$  is the gray level on each voxel, which is an integer between 0 and 255.

RANNOU J., LIMODIN N., RÉTHORÉ J., GRAVOUIL A., LUDWIG W., BAÏETTO -DUBOURG M.-C., BUFFIERE J.-Y., COMBESCURE A., HILD F., ROUX S.,  
Computer methods in applied mechanics and engineering, 199, 1307-1325, 2010.

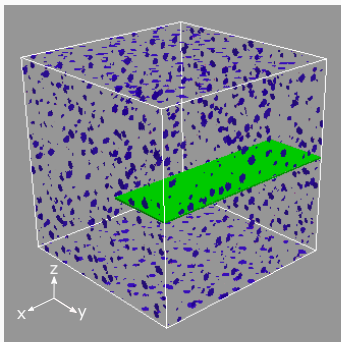


# CRACK OPENING IN CAST IRON

- Iron:  $E = 210$  GPa,  $\nu = 0.3$
- Carbon:  $E = 21$  GPa,  $\nu = 0.2$
- Size:  $L \times L \times L$
- Crack thickness: 3 voxels
- $Strain_o = 1\%$

Boundary conditions:

$$\begin{cases} u_z = 0, & \text{on } Z = -\frac{L}{2} \\ u_z = 0.01L, & \text{on } Z = \frac{L}{2} \\ \vec{u} = \vec{0}, & \text{at } (0,0,-\frac{L}{2}) \end{cases}$$



# CRACK OPENING

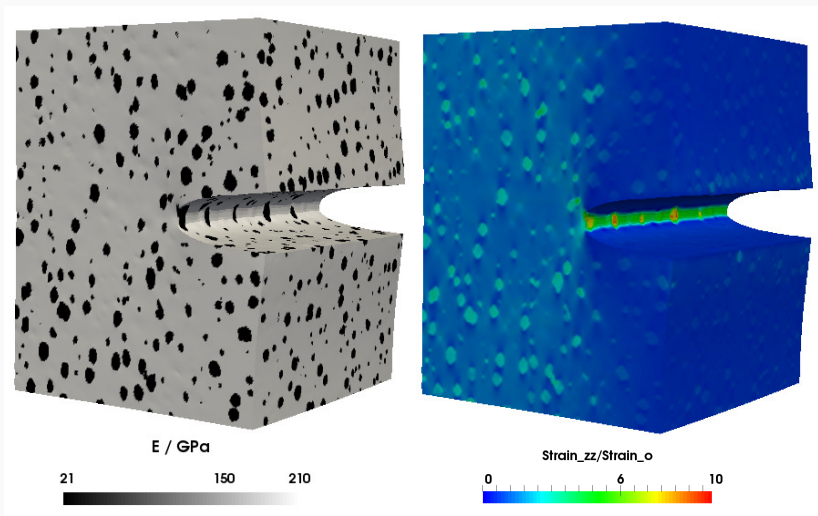


Figure 8: The Young's modulus and the  $\text{strain}_{zz}$  in cast iron. The displacement is multiplied by a factor of 20.

# CRACK OPENING

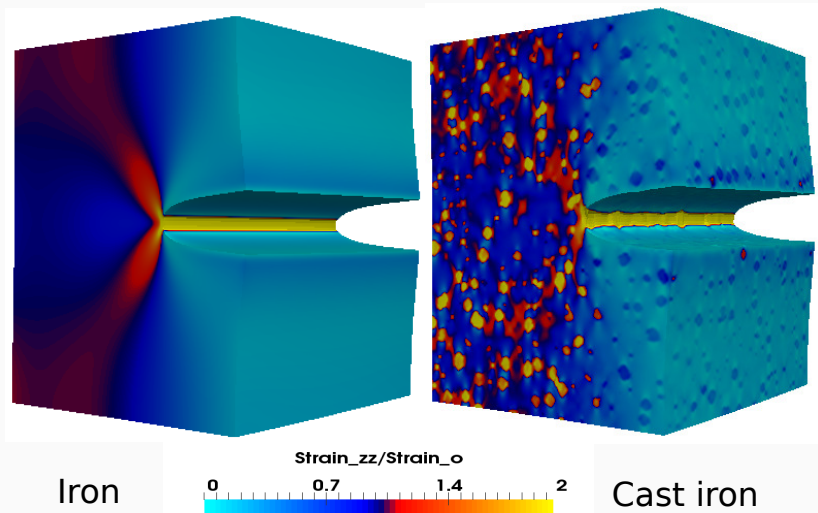


Figure 9: Strain<sub>zz</sub> in iron and in cast iron. The displacement is multiplied by a factor of 20.

## CRACK OPENING

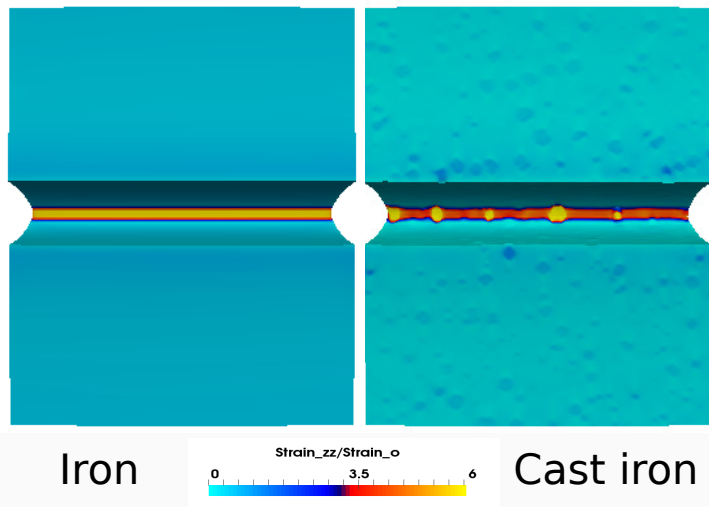
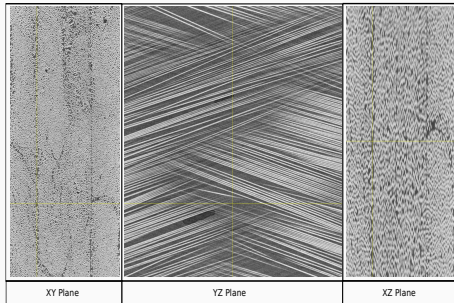


Figure 10: Strain concentrations on the crack front in the cast iron and in the iron. The displacement is multiplied by a factor of 20.

# LAMINATE COMPOSITE MATERIAL

The image of a composite material obtained by Lecomte-Grosbras et al.(2015): E-glass fiber with M9 epoxy resin

- $700 \times 1700 \times 1300$  voxels
- Four layers:  $15^\circ$ ,  $-15^\circ$ ,  $-15^\circ$  and  $15^\circ$



Lecomte-Grosbras, P., Réthoré, J., Limodin, N., Witz, J.-F., Brieu, M., 2015. Three-dimensional investigation of free-edge effects in laminate composites using x-ray tomography and digital volume correlation. *Experimental Mechanics* 55 (1), 301–311.

Experimental results obtained by digital image correlation (DIC)

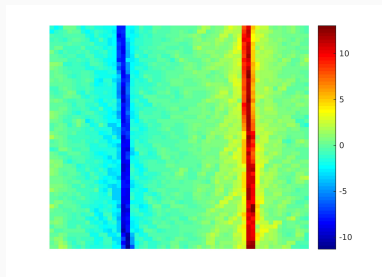
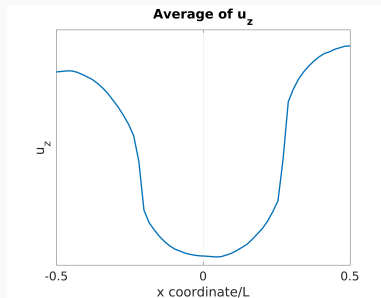


Figure 11: Strain<sub>xz</sub>

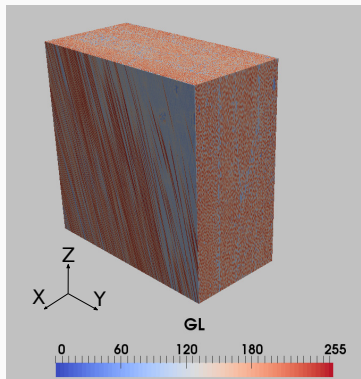


Free edge effects in this laminate structure

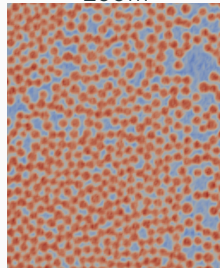
- Strain concentrations in the ply interface
- Large displacement gradient in the ply interface

# LAMINATE COMPOSITE MATERIAL

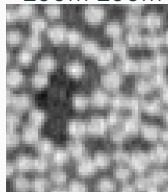
3D image



Zoom



Zoom Zoom



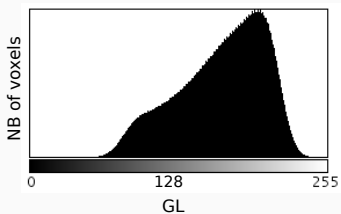
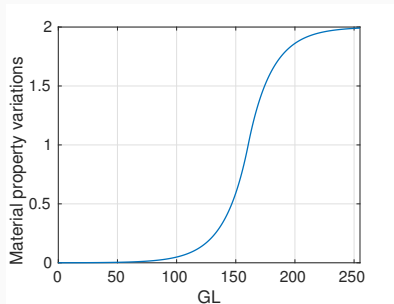


Figure 12: Histogram

Trial and error method

$$\alpha = \left(1 - e^{-\frac{|GL-160.5|}{20}}\right) \cdot \text{sign}(GL - 160.5) + 1$$





ROI:  $577 \times 1153 \times 1153$ , *i.e.* about 0.8 billion voxels

- E-glass fiber:  $E = 80.0$  GPa,  $\nu = 0.22$
- Epoxy:  $E = 3.2$  GPa,  $\nu = 0.22$

Subsampling into

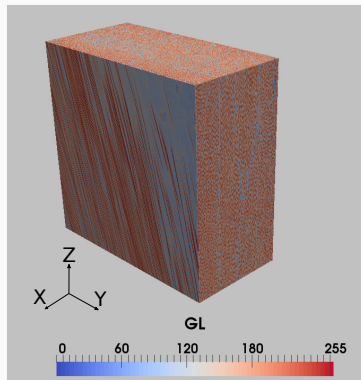
$1153 \times 2305 \times 2305$  voxels

$\approx 6$  billion voxels or 18 billion DoF.

Size:  $L \times 2L \times 2L$

$Strain_o = 1\%$

$$\begin{cases} \vec{u} = \{0, 0, -0.01L\}, & \text{on } z = -L \\ \vec{u} = \{0, 0, 0.01L\}, & \text{on } z = L \end{cases}$$



# NUMERICAL AND EXPERIMENTAL COMPARISON

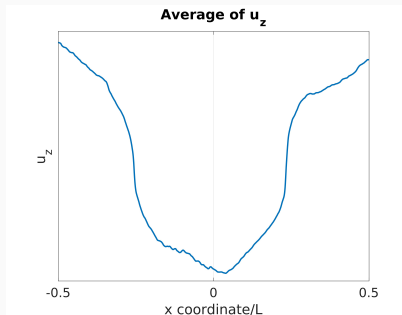


Figure 13: Numerical results

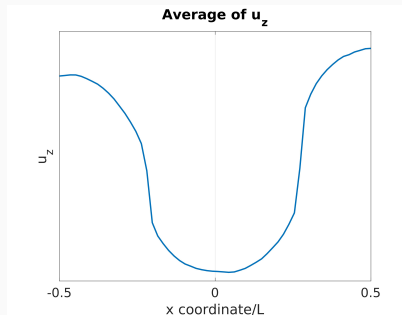
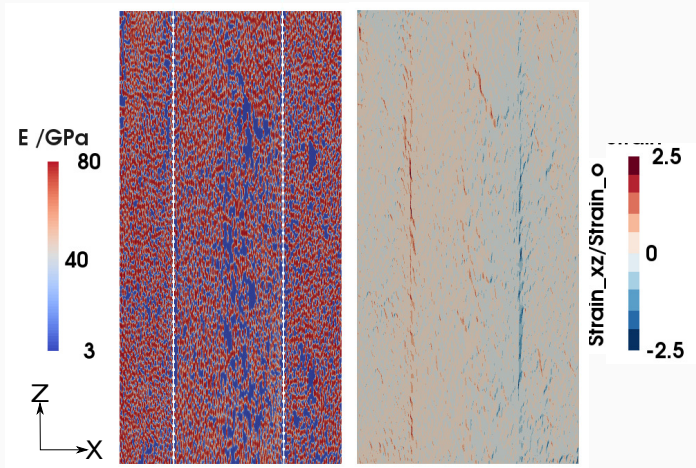


Figure 14: Experimental results

A good correlation can be found between the numerical simulation and the DIC experiment.

LECOMTE-GROSBRAS P, PALUCH B, BRIEU M, D E S AXC É G, SABATIER L, Composites Part A: Applied Science and Manufacturing, 40, 1911-1920, 2009.

# NUMERICAL RESULT



Strain concentrations in ply interface.

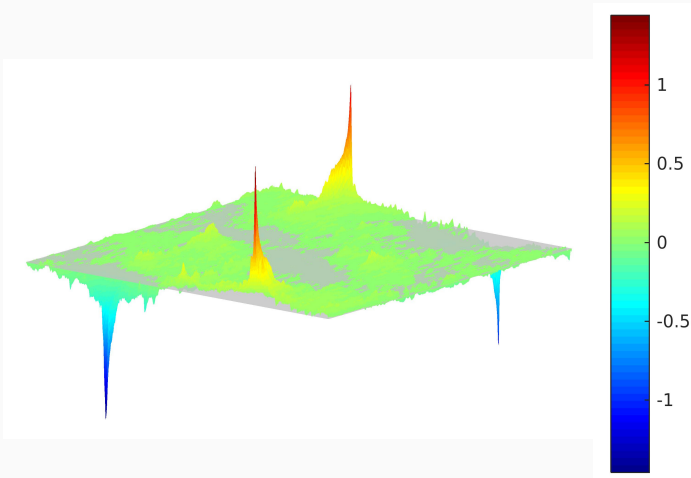


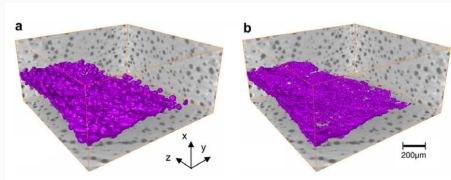
Figure 15: Averages of  $Strain_{xz}/Strain_o$  along axis Z

- The simulation with a large real tomography image (18 billion DoF) is performed
- The proposed strategy permits to analyze deformation mechanism at the microscopic scale
- The qualitative agreement between the simulation and the DIC experiment confirms the accuracy to perform CT simulations
- The interaction between the crack and the microstructure shows the indispensability to perform CT simulations

X. liu, J. Réthoré, M.-C. Baietto, P. Sainsot, A.-A. Lubrecht, An efficient strategy for large scale 3D simulation of heterogeneous materials to predict effective thermal conductivity, *Computational materials science*, 166, 265-275, 2019.

X. liu, J. Réthoré, M.-C. Baietto, P. Sainsot, A.-A. Lubrecht, A massively parallel matrix free finite element based multigrid method for simulations of the mechanical behavior of heterogeneous materials using large scale CT images, *Computational Mechanics*, online.  
IDS ConnectTalent project funded by Région Pays de la Loire and Nantes Métropole

- A quantitative comparison between the simulation and the DIC experiment is advised
  - Apply the measured boundary conditions
  - Identify real material property of each constitutive
- Phase field method to compute the crack propagation



- Up-scaling mechanical fields to incorporate crack /  $\mu$ structure interaction in a macroscale model. Elie EID PhD thesis, ANR JCJC METACRACK project.



# A MASSIVELY PARALLEL MATRIX FREE FE-BASED MULTIGRID METHOD FOR SIMULATING THE BEHAVIOR OF HETEROGENEOUS MATERIALS USING LARGE SCALE CT IMAGES

---

Xiaodong LIU, Julien RÉTHORÉ, Ton LUBRECHT

September 23, 2020

Research Institute in Civil Engineering and Mechanics (GeM)  
UMR 6183, CNRS, Centrale Nantes, Université de Nantes, France